NATURAL-ABUNDANCE CARBON-13 FOURIER TRANSFORM NMR STUDIES OF LARGE MOLECULES

ADAM ALLERHAND

Department of Chemistry, Indiana University, Bloomington, Indiana 47401, USA*

ABSTRACT

The resolution in proton-decoupled natural-abundance ^{13}C NMR† spectra of large organic and biological molecules is normally considerably greater than in proton NMR spectra, as a result of the large range of ^{13}C chemical shifts and the absence of $^{13}C—^{13}C$ coupling. The Fourier transform NMR technique has partly overcome the problem of very poor sensitivity of natural-abundance ^{13}C NMR.

As examples of structural applications, ^{13}C NMR has been used to determine the detailed anomeric composition of aqueous fructose, and to measure the extent and type of branching of various dextrans. Some problems that arise when ^{13}C Fourier transform NMR is used for quantitative analysis are discussed.

Fourier transform NMR instrumentation provides a built-in capability of measuring the spin–lattice relaxation time (T_1) of individual-carbon resonances. The meaning of T_1 and how spin–lattice relaxation occurs are briefly discussed. Examples of T_1 determinations are presented. The use of T_1 measurements for studying rotational motions of molecules and internal rotations of side-chains is discussed. PRFT NMR spectra can be used in some cases for assigning ^{13}C resonances to specific carbons.

The development of a probe for sample tubes of 20 mm outside diameter has increased the sensitivity of natural-abundance ^{13}C Fourier transform nuclear magnetic resonance to the point that single-carbon resonances of proteins can be studied. Numerous narrow single-carbon resonances are observed in the aromatic region of the ^{13}C spectrum of native hen egg-white lysozyme. Theoretical and experimental evidence shows that these narrow resonances are those of the 28 non-protonated aromatic carbons. The 59 protonated aromatic carbons give rise to a background of broad peaks. Significant chemical shift variations occur upon folding of the protein into its

* Contribution No. 2613.

† Abbreviations:

NMR, nuclear magnetic resonance
PRFT, partially relaxed Fourier transform
NOE, nuclear Overhauser enhancement
VLDL, very-low-density lipoprotein
LDL, low-density lipoprotein
HDL, high-density lipoprotein

native conformation. For example, the γ-carbons of the six tryptophan residues resonate at 81.4, 82.1, 83.2, 83.8 and 85.2 p.p.m. upfield from CS_2 (the peak at 85.2 p.p.m. is a two-carbon resonance). After denaturation with guanidinium chloride, all six carbons resonate at about 83.8 p.p.m. In the case of horse-heart ferrocytochrome *c*, not only the non-protonated aromatic carbons of amino acid residues but also those of the haem yield narrow resonances. Only those non-protonated aromatic carbons that are far away from the iron yield narrow resonances in the spectrum of the paramagnetic ferricytochrome *c*.

Applications of ^{13}C NMR in studies of lipoproteins and nucleic acids are also discussed.

INTRODUCTION

From the standpoint of sensitivity (minimum number of molecules necessary to detect a signal), NMR is the worst of all common spectroscopic techniques, as a result of the relatively small separations between the nuclear spin energy levels (even in the highest magnetic field strengths available today). In spite of this handicap, the ability of high-resolution NMR to monitor the environments of individual atomic sites of molecules in solution has generated a remarkably wide range of applications for this spectroscopic technique. The information content in *proton* NMR spectra gradually diminishes as the size and complexity of the molecule increases. Ideally, one wishes to observe and assign a *resolved* resonance for *each* non-equivalent hydrogen of a molecule. In practice, there are two factors that conspire against such an ideal situation. First, the range of ^1H chemical shifts is only about 10 p.p.m. (1000 Hz in a magnetic field of 23.5 kG). Second, scalar coupling between non-equivalent hydrogens (homonuclear coupling) produces splitting of the resonances. Consequently, the number of resonances is usually considerably greater than the number of non-equivalent hydrogens. I like to define 'resonance density' as the average number of resonances per p.p.m. As a result of the small range of ^1H chemical shifts and of the splittings caused by homonuclear coupling, ^1H NMR spectra of most natural products and other large organic molecules have a high resonance density. Therefore, the spectral resolution is often poor, unlike the situation with small organic molecules. As an example, consider the medium-size molecule phytol (*Figure 1*). The ^1H NMR spectrum of phytol, even when recorded at 51.7 kG (220 MHz), is basically a featureless 'blob' (*Figure 2*). In contrast, the proton-decoupled (see below) natural-abundance ^{13}C NMR spectrum of phytol yields resolved single-carbon resonances for 18 out of the 20 carbons[1] (*Figure 3*), even when recorded at only 14.2 kG (15.18 MHz). This is not an isolated case: the proton-decoupled natural-abundance ^{13}C NMR spectra of practically all types of large organic molecules show a high degree of resolution. Vitamin B_{12} and other corrinoids[2], chlorophyll *a*[1,3,4] (*Figures 4* and *5*), steroids[5], and carbohydrates[6–8] are examples of types of molecules

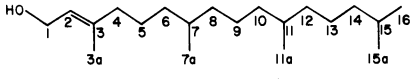

Figure 1. Structure of phytol

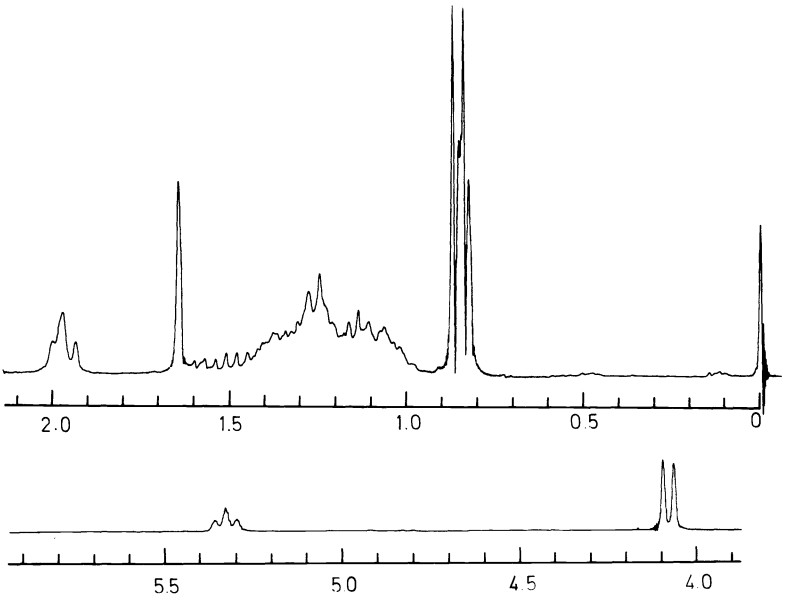

Figure 2. Continuous-wave proton NMR spectrum of 0.68 M phytol in $CDCl_3$ (plus tetramethylsilane), recorded at 220 MHz (in a 5 mm tube) with a single scan. Horizontal scale is in p.p.m. downfield from internal Me_4Si

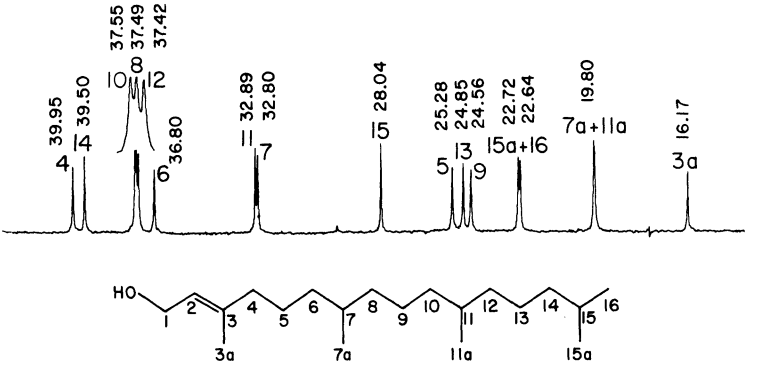

Figure 3. Bottom: Structure of phytol. Top: Upfield region (about 14 p.p.m. to about 43 p.p.m. downfield from Me_4Si) in the proton-decoupled natural-abundance ^{13}C Fourier transform NMR spectrum of 0.55 M phytol in chloroform at 48°, recorded at 15.18 MHz (in a 20 mm tube) with a 1000 Hz spectral width, 16384 points in the time domain (0.122 Hz digital resolution) and 32 accumulations with a recycle time of 31.6 s. The insert shown above some resonances was printed with a fourfold expansion of the horizontal scale. The larger numbers in the spectrum are assignments to specific carbons[1]. The smaller numbers are chemical shifts in p.p.m. downfield from internal Me_4Si

that yield highly resolved ^{13}C NMR spectra. Why is this so? First, the range of ^{13}C chemical shifts is greater than that of ^{1}H chemical shifts. Second (and perhaps more important) is the lack of splittings from homonuclear (^{13}C—^{13}C) scalar couplings. This is a consequence of the low natural abundance of the ^{13}C isotope, which results in a low percentage of molecules with two or

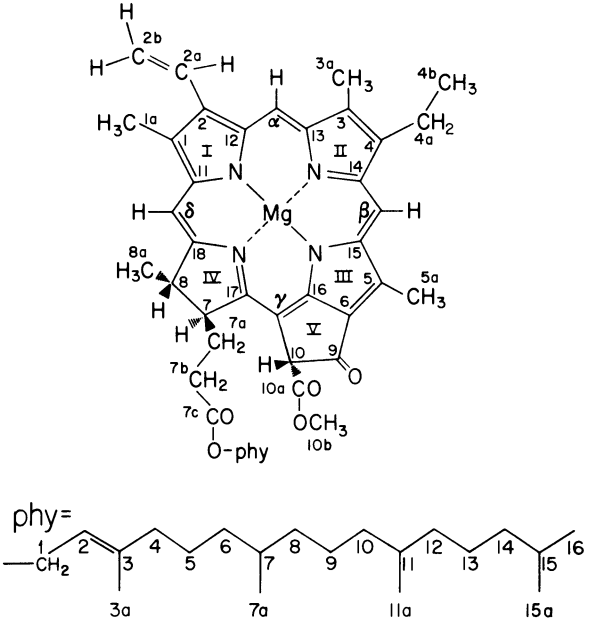

Figure 4. Structure of chlorophyll *a*

more ^{13}C nuclei in the same molecule. Therefore, the only type of scalar coupling that we have to worry about is *heteronuclear* coupling, which can always be eliminated by strong irradiation at the resonance frequency of the other nucleus. In fact, ^{1}H decoupling, pioneered by Grant[9], is routinely carried out in recording ^{13}C NMR spectra. The ^{13}C NMR spectra presented in this paper were recorded in the presence of sufficiently strong irradiation at the resonance frequencies of all the ^{1}H nuclei to cause saturation (equalization of populations) of the ^{1}H energy levels. Note that I have referred to the ^{1}H resonance *frequencies*. The frequency of the decoupling irradiation is usually random noise modulated to cover the whole range of ^{1}H chemical shifts. Under conditions of proton decoupling, natural-abundance ^{13}C NMR spectra are basically very simple: each carbon normally gives rise to one peak (except when splitting occurs as a result of scalar coupling to some nucleus other than ^{1}H, such as ^{31}P).

On the basis of the above considerations and examples, it is obvious that ^{13}C NMR can be very useful for structural elucidations of large organic molecules. This has been known for many years, largely as a result of the

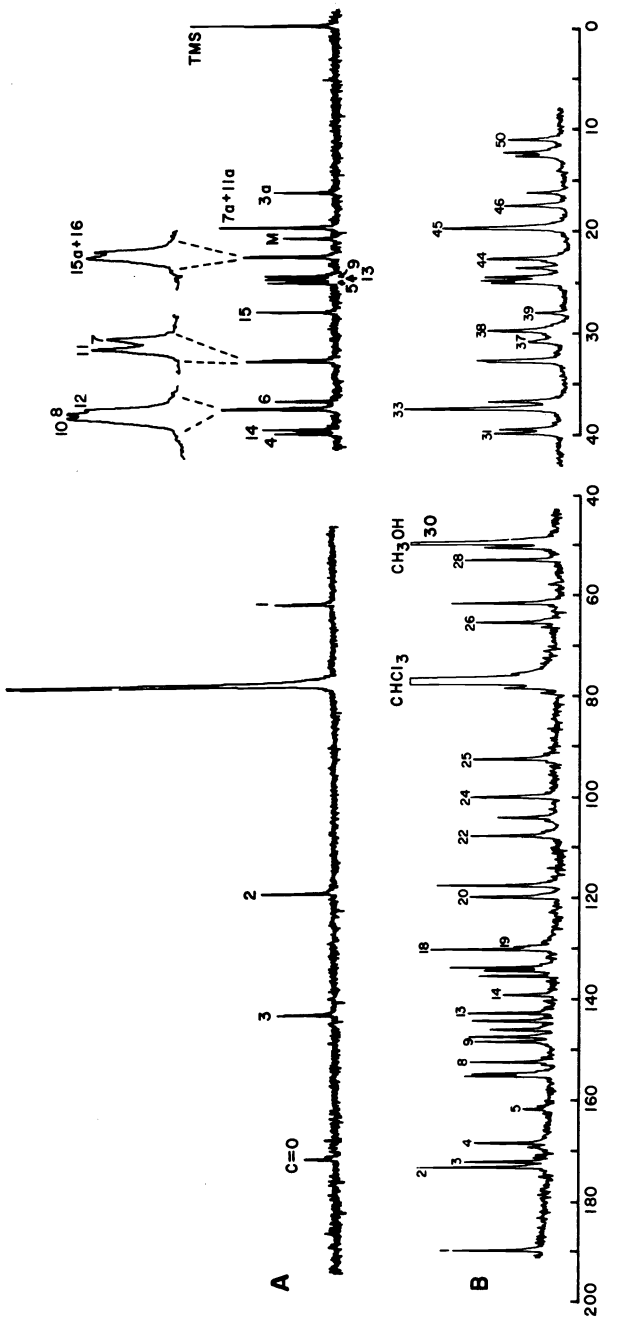

Figure 5. Proton-decoupled natural-abundance ^{13}C Fourier transform NMR spectra recorded at 15.18 MHz with a 20 mm sample tube. (A) Spectrum of 0.56 M phytyl acetate in chloroform (with Me_4Si), recorded at 60°, 16 accumulations with a recycle time of 90 s, and 16 384 points in the time domain being used. Spectral widths of 3048.78 Hz (0.372 Hz digital resolution) and 1000 Hz (0.122 Hz digital resolution) were used for the downfield region and upfield region, respectively. Phytyl peak assignments are given using the carbon designations of *Figures 1* and *4*. Peak M is the acetate methyl carbon resonance. The inserts shown above some peaks were printed with an eightfold expansion of the horizontal scale. (B) Spectrum of 1.45 g chlorophyll *a* in 7.9 ml chloroform and 0.6 ml methanol, recorded at 35°, after 1024 accumulations with 4096 points in the time domain, spectral widths of 250 p.p.m. (downfield) and 62.5 p.p.m. (upfield), and recycle times of 8.44 s (downfield) and 2.32 s (upfield) being used

pioneering work of Lauterbur[10], Grant[9, 11] and Roberts[5, 12]. A vast literature on ^{13}C chemical shifts has accumulated[13]. Nevertheless, it is only in the last few years that ^{13}C NMR has become an attractive technique for studying large molecules, mainly as a result of the introduction of commercial Fourier transform NMR spectrometers.

Because of the extremely poor sensitivity of natural-abundance ^{13}C NMR, a single spectral scan does not yield observable peaks except in those fortunate cases when the concentration is very high ($\gtrsim$1 M). Therefore, ^{13}C NMR spectrometers are equipped with an analogue-to-digital converter and a digital memory for the purpose of digitizing every scan and adding the signals from repetitive scans. The accumulated signal grows linearly with the number of scans, while the noise grows as the square root of the number of scans. Therefore, the ultimate signal-to-noise ratio is proportional to the square root of the number of scans. With a typical commercial NMR spectrometer, about 20000 scans are required to get a useful natural-abundance ^{13}C spectrum of a 10 mM solution of an organic molecule[14]. If one uses an 'old-fashioned' continuous-wave n.m.r. spectrometer, each scan takes about 100 s (or more). About 3 weeks would be needed to get a ^{13}C spectrum of a 10 mM solution. Only 14 spectra per year would result, if the spectrometer operated continuously without breakdowns and wear and tear!

If one uses a commercial Fourier transform NMR spectrometer[15], then each scan requires only about 1 s, and it is possible to get a useful ^{13}C spectrum of a 10 mM solution in about 10 h of signal accumulation time[14]. With additional instrumental improvements developed in my laboratory[16] (see below), a ^{13}C spectrum of a 10 mM solution can be obtained in 30 min of signal averaging (*Figure 6*), and the lowest practical concentration for natural-abundance ^{13}C NMR studies of large organic molecules is about 1 mM[16].

I present below some typical applications of proton-decoupled natural-

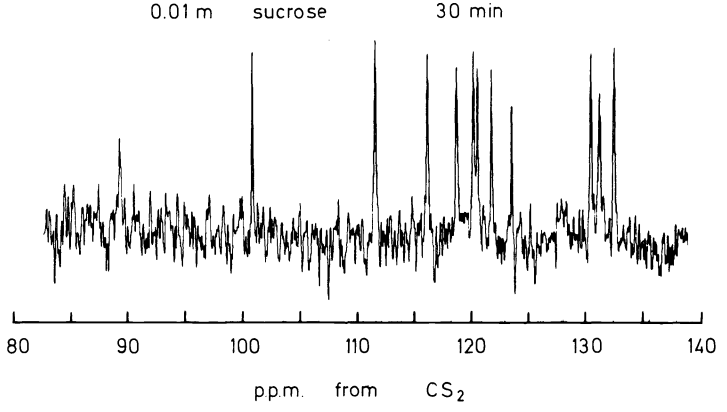

Figure 6. Proton-decoupled natural-abundance ^{13}C Fourier transform NMR spectrum of 0.01 M aqueous sucrose at about 50°, recorded at 15.18 MHz in a 20 mm sample tube, 90° rf pulses, 8192 points in the time domain, a spectral width of 2500 Hz, a recycle time of 1.755 s and 1024 accumulations (30 min total time) being used. A digital line broadening of 1.17 Hz was applied in order to improve the signal-to-noise ratio

abundance ^{13}C Fourier transform NMR spectra. Numerous important applications of ^{13}C NMR have been reported in the last few years by many workers. The examples presented below are from my laboratory. All the spectra were recorded by the Fourier transform method, at 15.18 MHz. With the exception of some spectra of neat phytol, the results were obtained with the use of our 20 mm probe[16]. Except for our results on biopolymers, the same information could have been obtained (in a practical amount of time) with the use of typical commercial Fourier transform NMR spectrometers.

MOLECULAR STRUCTURE

Anomeric equilibria of ketoses

Proton NMR has been used to study anomeric equilibria of aldoses in aqueous solution[17] by observing the relatively isolated downfield resonance of the hydrogen attached to the anomeric carbon. Proton NMR has not been used to study anomeric equilibria of ketoses such as fructose, because the anomeric carbon is non-protonated, and as a result there are no easily assignable ^{1}H resonances (*Figure 7*). Carbon-13 NMR is very suitable in this

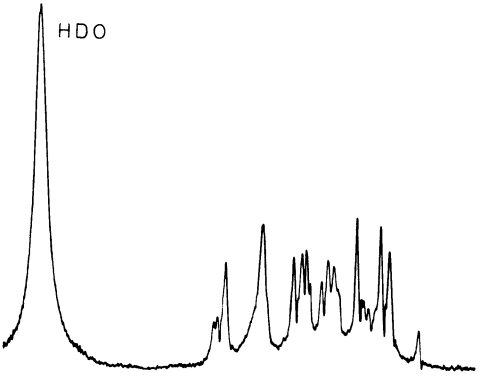

Figure 7. Continuous-wave proton NMR spectrum of the equilibrium anomeric mixture of D-fructose (0.5 M) in D_2O at about 30°, recorded at 100 MHz in a 5 mm tube, with a single scan. A spectral width of 1.46 p.p.m. is shown

case. Only a few minutes of signal accumulation are needed to get a high signal-to-noise ratio in the ^{13}C spectrum of a concentrated solution of aqueous fructose (*Figure 8*). A spectrum obtained immediately after dissolving β-D-fructose in water shows mainly the six resolved resonances of the carbons of β-D-fructopyranose[7] (*Figure 8A*), which is the anomeric form of the crystalline material[18]. Several hours later the spectrum of the equilibrium anomeric mixture is obtained (*Figure 8B*). This spectrum clearly shows the presence of four anomers[7]. Chemical shifts of model compounds yield specific assignments of most of the resonances[19, 20]. Spectral intensities yield the detailed anomeric composition[7]. Carbon-13 NMR appears to be the only method available today for determining the anomeric composition of ketoses which

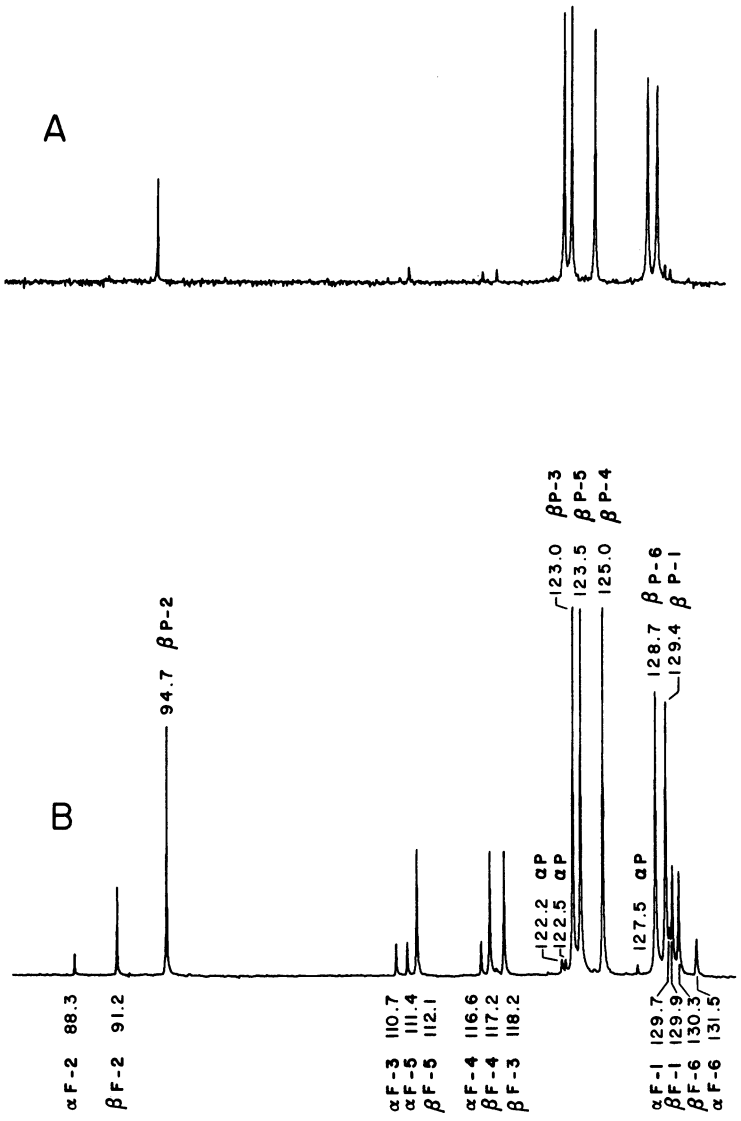

Figure 8. Proton-decoupled natural-abundance ^{13}C Fourier transform NMR spectra of aqueous D-fructose (270 g/l solution) at about 35°, recorded at 15.18 MHz, with a 2000 Hz spectral width and a recycle time of 6 s. A digital broadening of 0.155 Hz was applied to each spectrum in order to improve the signal-to-noise ratio. (A) Spectrum recorded immediately after dissolving D-fructose, 16 accumulations (1.6 min total time) and 8192 time-domain points being used. 16 384 time-domain points were used for the Fourier transformation, by placing 8192 blank addresses at the tail end of the accumulated signal. (B) Spectrum recorded about 8 h after dissolving D-fructose, 570 accumulations (about 1 h total time) and 16 384 time-domain points being used. Chemical shifts are given in p.p.m. upfield from CS_2. Details have been given elsewhere[7]. Assignments are those of Que and Gray[19] and Doddrell and Allerhand[7]. F = D-fructofuranose: P = D-fructopyranose; αF-2 = carbon 2 of α-D-fructofuranose

yield more than two anomers in solution. Compare the simplicity and ease of interpretation of the ^{13}C spectrum of *Figure 8B* with the hopeless ^{1}H spectrum of *Figure 7*!

Branching of dextrans

Dextrans are a group of polysaccharides of high molecular weight synthesized by various microorganisms. The most important dextrans are produced from sucrose by the action of various strains of *Leuconostoc mesenteroides*[21]. These dextrans are mainly linear chains of $1 \rightarrow 6'$ linked α-D-glucopyranose units. The various strains of *Leuconostoc mesenteroides* yield dextrans which differ in the degree of branching and in the nature of the linkages at the branching points ($1 \rightarrow 3'$, $1 \rightarrow 4'$ and $1 \rightarrow 2'$). Traditionally, chemical degradation methods have been used for determining the degree of branching and the nature of the linkages at the branching points[21]. Conflicting results have often resulted from various degradation procedures, probably as a consequence of side reactions. Carbon-13 NMR is a good non-destructive technique for studying branching characteristics of dextrans[22,23]. *Figure 9* presents ^{13}C spectra of aqueous solutions of several dextrans. All the spectra have six strong resonances that arise from the $1 \rightarrow 6'$ linked α-glucopyranose units of the main chain. All the spectra also have a peak (at 132.2 p.p.m. in *Figure 9*) that can be assigned to unlinked CH_2OH groups[6]. A comparison of the integrated intensity of this peak with that of the main C-6 resonance (at 127.2 p.p.m. in *Figure 9*) yields quantitative information about the extent of branching[23], because the presence of each $—CH_2OH$ group is the result of one branch point. We can neglect the $—CH_2OH$ group at one end of the main chain, because of the high molecular weights involved here. Quantitative information about the *type* of branching can be extracted from the integrated intensities of the minor peaks at 111.9 p.p.m., 114.3 p.p.m. and 117.2 p.p.m. in *Figure 9*. These resonances arise from carbons 3, 4 and 2, respectively, when these carbons participate in a glycosidic linkage. Details are given elsewhere[23].

Precautions in quantitative analysis

We have discussed above two examples of applications of ^{13}C NMR to quantitative analysis. These applications require judicious use of ^{13}C signal intensities. Insufficient digital resolution, differences in spin–lattice relaxation times (T_1) and differences in nuclear Overhauser enhancements (NOE) can produce serious errors in quantitative analysis by means of ^{13}C NMR. We will now discuss each of these three factors.

Figure 10 shows the proton-decoupled natural-abundance ^{13}C resonance of neat ethylene glycol at about 36°, in a 20 mm sample tube[16]. The observed linewidth is 0.64 Hz. The natural linewidth of neat ethylene glycol at 36° (inferred from T_1 measurements) is about 0.3 Hz, so that the observed linewidth has a contribution of about 0.3–0.4 Hz from magnetic field inhomogeneity. The spectrum of *Figure 10* was recorded with a digital resolution of 0.05 Hz. The open and solid circles of *Figure 10* are the digital values taken from the computer memory. The solid circles are spaced 0.5 Hz apart, and the solid line that joins them gives one example of a lineshape that would be obtained under conditions of 0.5 Hz digital resolution. Clearly, 0.05 Hz

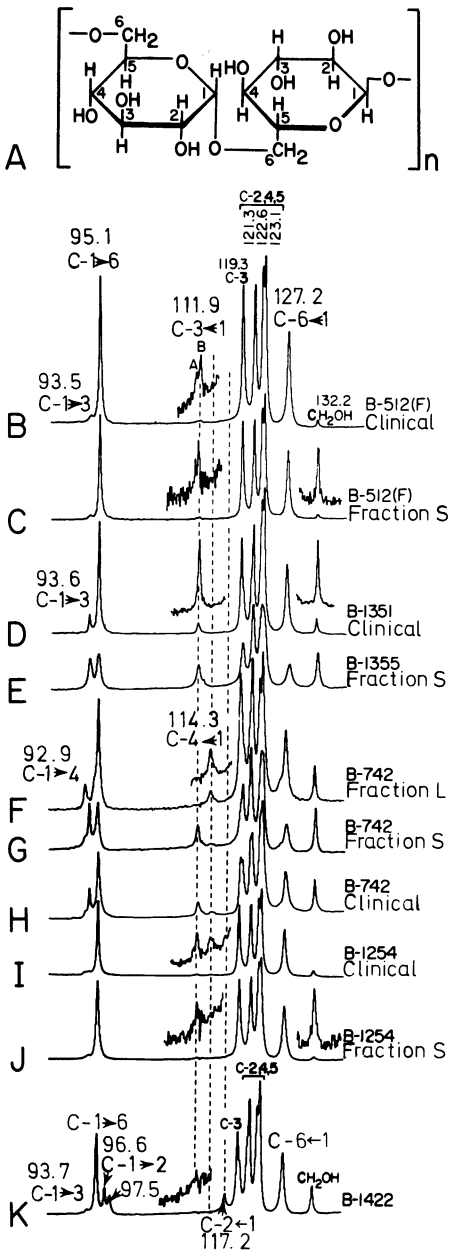

Figure 9. (A) Structure of linear chain of dextrans. (B)–(K) Proton-decoupled natural-abundance ^{13}C Fourier transform NMR spectra of aqueous dextrans at about 50°, recorded at 15.18 MHz in 20 mm tubes, with 125 p.p.m. spectral widths and 2048 time-domain points. Chemical shifts are in p.p.m. from CS_2. Concentrations (g/l H_2O), recycle times (s) and number of scans were: (B) 198, 0.574, 24 576; (C) 169, 0.543, 15 360; (D) 139, 0.543, 16 384; (E) 107, 0.543, 20 480; (F) 63, 0.543, 24 576; (G) 63, 0.553, 49 152; (H) 193, 0.543, 16 384. (I) 188, 0.543, 32 768; (J) 69, 0.553, 57 344; (K) 150, 0.543, 16 384

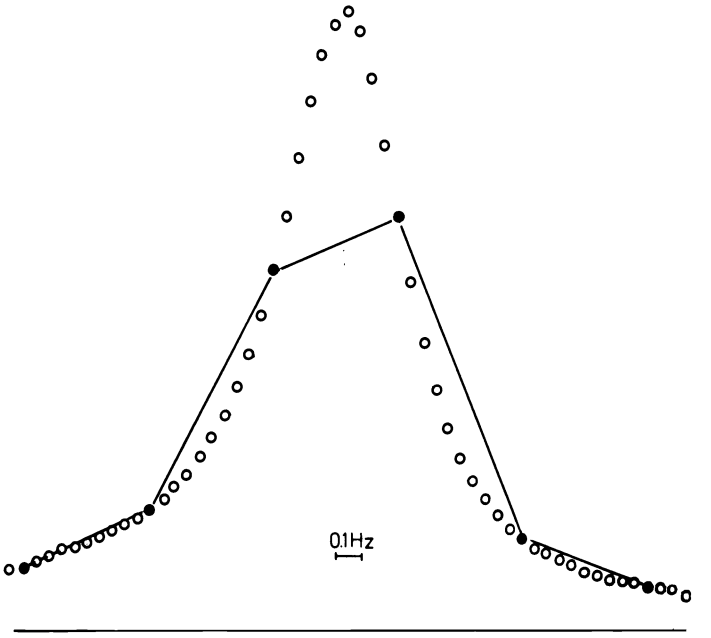

Figure 10. Single-scan, proton-decoupled natural-abundance ^{13}C Fourier transform NMR spectrum of neat ethylene glycol at about 36°, recorded at 15.18 MHz in a 20 mm tube, with a 90° rf pulse, a spectral width of 409.5 Hz and 16384 time-domain addresses (0.05 Hz digital resolution). The circles are the experimental digital values for the lineshape (spaced 0.05 Hz apart). The solid circles are spaced 0.5 Hz apart, and the line that joins them gives an example of a lineshape that would have resulted with the use of 0.5 Hz resolution

digital resolution gives much better peak definition than 0.5 Hz resolution. In order to cover the complete range of ^{13}C chemical shifts, one normally needs a spectral window of about 200 p.p.m. or more[13, 14], which is about 3000 Hz and 5000 Hz at 14.1 kG and 23.5 kG, respectively. We would need a computer memory of 100000 addresses to store a 5000 Hz spectrum with a resolution of 0.05 Hz (actually, 200000 addresses would be needed to store the time-domain signal[15]). It is not surprising that ^{13}C Fourier transform NMR spectra are normally recorded with a resolution of about 0.5 Hz or even 1 Hz. Consequently, if the resonances are narrow (linewidth $\lesssim 2$ Hz), poor digital definition can seriously limit the accuracy of integrated intensities. If the resonances are well separated, it is desirable (and easy) to broaden them by means of digital processing[15, 24], in order to improve peak definition.

When two carbons have different spin–lattice relaxation times (T_1), then their resonances may have different intensities, if the recycle time (interval between successive pulses of radiofrequency excitation) is not much greater than the T_1 values[15]. In the next section we will show how to measure T_1 values, and how to extract useful information from such measurements. We will start here with a qualitative explanation of spin–lattice relaxation.

When placed in a magnetic field, a spin–$\frac{1}{2}$ nucleus (such as ^{1}H, ^{13}C, ^{15}N, ^{19}F, ^{29}Si, ^{31}P, and others) has two energy states. Assume that you have

placed your sample in a magnetic field, and that you have waited long enough for the populations of the two spin states to reach their equilibrium values. Suppose now that you change the populations to a non-equilibrium distribution (by means of a pulse of radiofrequency excitation, for example). If left to its own devices, the spin system will try to reach the equilibrium populations, in an exponential or nearly exponential manner in most cases. When the decay is exponential (as in ^{13}C relaxation under conditions of proton decoupling[25]), we can define a time constant $1/T_1$ for this decay. T_1 is called the spin–lattice (or longitudinal) relaxation time. Different carbons within the same molecule may have very different T_1 values (see next section). If two carbons have different T_1 values, and if the recycle time is not much longer than both T_1 values, then the carbon with the longer T_1 value will yield a weaker resonance than the other one[15]. Clearly, in the absence of T_1 information it is dangerous to use the relative intensities of ^{13}C resonances for quantitative analysis of mixtures.

The nuclear Overhauser enhancement (NOE) is an increase in the intensity of a ^{13}C resonance as a result of proton-decoupling[26]. Different carbons may have different NOE values[25]. Clearly, a knowledge of the NOE is necessary before one can use the relative intensities of ^{13}C resonances for quantitative analysis of mixtures. The NOE arises from a redistribution of the populations of the ^{13}C energy levels upon proton irradiation. The ^{13}C resonances of *protonated carbons of large organic molecules* normally have the maximum NOE of 2.988[26, 27]. In other words, the signal intensity in the presence of proton decoupling is three times greater than in the absence of ^{1}H irradiation.

Two conditions must be satisfied in order to observe the full NOE of 2.988. First, ^{13}C relaxation must occur entirely by $^{13}C—^{1}H$ dipole–dipole interactions (see next section). If other relaxation mechanisms are important, the NOE is reduced[25, 26]. Second, the effective correlation time for rotational reorientation (τ_{eff}) of the vectors connecting the ^{13}C nucleus to the ^{1}H nuclei that cause dipolar relaxation must be small relative to the proton resonance frequency (ω_H) in rad/s[26, 28]:

$$\tau_{eff}\omega_H \ll 1 \qquad (1)$$

This 'extreme narrowing condition' is normally satisfied for organic molecules, because their correlation time for over-all rotational reorientation (τ_R) in solution is usually in the range 10^{-12}–10^{-10} s. In the case of biopolymers in their native conformation, τ_R is typically 10^{-8} s or greater, and equation 1 will not be satisfied, unless τ_{eff} is dominated by fast internal reorientations[28, 29].

A common misconception is that non-protonated carbons of organic molecules should have one-third the intensity of protonated carbons. This can only happen if the $^{13}C—^{1}H$ dipolar relaxation mechanism (see next section) makes a negligible contribution to the relaxation of the non-protonated carbons. It is true that $^{13}C—^{1}H$ dipolar relaxation is much weaker for non-protonated carbons than for protonated ones (see next section). However, the $^{13}C—^{1}H$ dipolar relaxation mechanism *can* be the dominant one even for non-protonated carbons[27]. In fact, examples of non-protonated carbons with an NOE of about 3 have been reported[27].

It is safe to assume that protonated carbons of large organic molecules (in the absence of paramagnetic centres) have the full NOE of 2.988. Therefore, differential NOE effects will not complicate the use of the resonances of such

carbons in quantitative analysis. Differential NOE effects may be present when we deal with non-protonated carbons, or with very small molecules (where the spin–rotation mechanism may dominate ^{13}C relaxation, as in the case of cyclopropane[30]), or with very large rigid molecules (such as biopolymers[28, 29]) or with paramagnetic species.

MOLECULAR MOTIONS

The Fourier transform NMR method not only overcomes, to some extent, the poor sensitivity of ^{13}C NMR. It provides a bonus: a Fourier transform NMR spectrometer can have, at practically no additional cost, the built-in capability of conveniently measuring the spin–lattice relaxation time of each resonance. We can conveniently measure the T_1 value of every ^{13}C nucleus that yields a resolved resonance by the PRFT method[27]. First we *invert* populations by means of a 180° radiofrequency pulse[24]. Then we wait an interval τ before applying the 90° radiofrequency pulse that generates the observed signal[24]. If the waiting interval τ is very much longer than the T_1 of a particular ^{13}C nucleus, then equilibrium of populations will be reestablished before the application of the 90° pulse, and we will get an 'ordinary' spectrum, as if the 180° pulse had not been applied: each resonance will have its equilibrium intensity A_∞. If the waiting interval τ is very much shorter than T_1, then the observing 90° pulse will be applied under conditions of inverted populations, and we will get an 'inverted' spectrum with 'negative' peaks of equal amplitude to the 'positive' peaks that would have resulted in the absence of population inversion. The amplitude A_τ of a resonance in a 'partially relaxed' Fourier transform (PRFT) spectrum generated as described above is given by[24]

$$A_\tau = A_\infty[1 - 2\exp(-\tau/T_1)] \tag{2}$$

A resonance will be 'negative' if τ is smaller than $T_1 \ln 2$ and 'positive' if τ is larger than $T_1 \ln 2$. In principle, it is possible to measure T_1 by finding the value of τ (τ_{null}) that yields no signal at all. It follows from equation 2 that $\tau_{null} = T_1 \ln 2$. In practice, more accurate T_1 values are obtained from a series of PRFT spectra with different values of τ. A plot of $\ln(A_\infty - A_\tau)$ versus τ should be linear with a slope $-1/T_1$.

Some ^{13}C PRFT spectra of phytol (*Figure 1*) are shown in *Figure 11*. The resulting T_1 values are given in *Figure 12*. The T_1 value of each protonated carbon has been multiplied by the number of directly bonded hydrogens (see below).

Now that we have established that T_1 values of individual ^{13}C resonances can be measured on practically any Fourier transform NMR spectrometer, we are ready to discuss the purpose of T_1 measurements. Carbon-13 spin–lattice relaxation times yield information about over-all molecular rotations and internal motions within molecules[25–33]. They can also be used for assigning ^{13}C resonances to specific carbons[1, 2, 8, 27, 32]. All these applications require an understanding of ^{13}C relaxation mechanisms.

As discussed above, ^{13}C spin–lattice relaxation involves transitions between the two spin states of a ^{13}C nucleus placed in a magnetic field. We are *not* talking here about transitions induced by an instrumentally

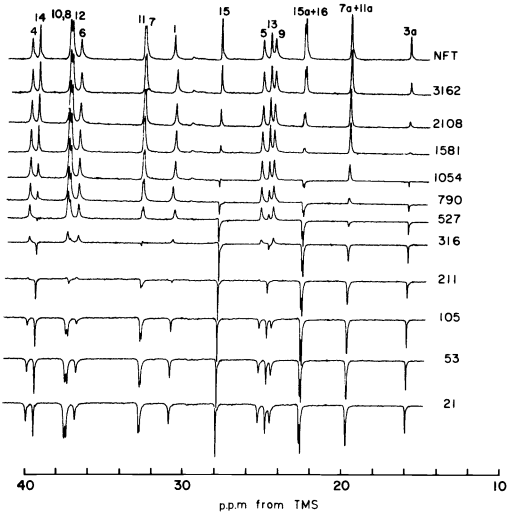

Figure 11. Upfield region of some proton-decoupled natural-abundance ^{13}C PRFT NMR spectra of neat phytol at 52°, recorded at 15.18 MHz in a 13 mm tube, with a spectral width of 31.25 p.p.m., 4096 points in the time domain, 64 accumulations and a recycle time of about 10 s. The normal spectrum (NFT) is shown at the top, with assignments of the resonances shown above each peak. Because of the small spectral width used here, the resonance of C-1 (at about 60 p.p.m.) is 'folded' to about 31 p.p.m. The number next to each PRFT spectrum is τ (the interval between a 180° rf pulse and the following 90° pulse), in ms.

applied radiofrequency excitation, but transitions that occur in the absence of any external radiofrequency irradiation. Spin–lattice relaxation is produced by electromagnetic radiation generated within the sample (we are interested here only in the magnetic component, because n.m.r. excitation involves magnetic dipole transitions). There must be some internal source of electromagnetic radiation, built-in within the sample, that has a non-zero amplitude at the ^{13}C resonance frequency. It is necessary to consider the various interactions that fluctuate in strength, and to compute how much intensity the resulting fluctuating magnetic field has at the resonance frequency. A relatively simple situation occurs in the case of *protonated* carbons of large molecules (in the absence of paramagnetic species): only one relaxation mechanism is important, the so-called $^{13}C—^{1}H$ dipole–dipole relaxation mechanism[27].

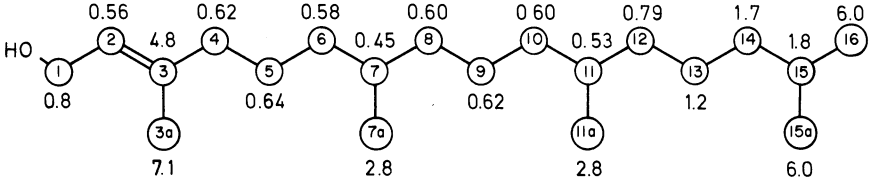

Figure 12. NT_1 map for neat phytol at 52°. The values of NT_1 (large numbers, in s) are shown for all carbons except for C-3, whose T_1 value is indicated. Small numbers are carbon designations of *Figure 1*

The strength of the dipole–dipole interaction between two spins is a function of the angle between the external magnetic field and the vector connecting the two spins. Therefore, over-all rotational motion of the molecule and internal rotations of C—H vectors will produce fluctuations of the dipole–dipole interaction. It can be shown[25] that in the case of a protonated carbon which is part of a rigid molecule undergoing isotropic rotation, the resulting T_1 value is given by

$$10(NT_1)^{-1} = (h/2\pi)^2\gamma_H^2\gamma_C^2 r^{-6}\chi \tag{3}$$

Here N is the number of directly bonded hydrogens, γ_H and γ_C are the gyromagnetic ratios of ^1H and ^{13}C, r is the C—H bond length and χ is defined by equation 4:

$$\chi = \frac{\tau_R}{1 + (\omega_H - \omega_C)^2\tau_R^2} + \frac{3\tau_R}{1 + \omega_C^2\tau_R^2} + \frac{6\tau_R}{1 + (\omega_H + \omega_C)^2\tau_R^2} \tag{4}$$

ω_H and ω_C are the resonance frequencies of ^1H and ^{13}C, respectively, in rad/s, and τ_R is the correlation time for rotational reorientation. Typical values of τ_R for organic molecules in common solvents are in the range 10^{-12}–10^{-9} s at room temperature. The τ_R values of organic molecules, but not those of biopolymers, satisfy the extreme narrowing condition (equation 1). When this condition applies, equation 3 becomes

$$(NT_1)^{-1} = (h/2\pi)^2\gamma_H^2\gamma_C^2 r^{-6}\tau_R \tag{5}$$

Equation 5 predicts an increase in T_1 as the rate of molecular tumbling increases (τ_R decreases).

A measurement of T_1 of a protonated carbon yields a value of τ_R. When equation 5 does not apply, it is sometimes useful to write

$$(NT_1)^{-1} = (h/2\pi)^2\gamma_H^2\gamma_C^2 r^{-6}\tau_{eff} \tag{6}$$

Here τ_{eff} is an 'effective' rotational time for the pertinent C—H vector. Equation 6 must be used with caution, because τ_{eff} may be a complicated (and often unknown) function of many degrees of rotational freedom. Where there are few degrees of rotational freedom, such as in the case of a methyl group undergoing internal rotation while attached to a rigid molecule which rotates isotropically, it is preferable to derive the *exact* relationship between T_1 and the various rotational correlation times[25, 27, 31].

It should be noted that the contribution of dipole–dipole relaxation to $1/T_1$ is proportional to the inverse of the sixth power of the distance between the nuclei involved. Therefore, the ^{13}C—^1H dipolar relaxation mechanism is much less effective for non-protonated carbons than for protonated ones. Non-protonated carbons usually have relatively long relaxation times[27]. Also, contributions from relaxation mechanisms other than the ^{13}C—^1H dipolar one can be significant for non-protonated carbons[25].

We will now consider two examples of ^{13}C T_1 studies: gramicidin S (in methanol) and phytol (neat liquid).

The ^{13}C spectrum of gramicidin S in methanol is shown in *Figure 13*[31]. The molecular structure and values of NT_1 are given in *Figure 14*[31]. The T_1 values of the α-carbons can be introduced into equation 5 to get the correlation

time for the *over-all* rotation of gramicidin S in methanol. The resulting τ_R value is $(3.3 \pm 0.2) \times 10^{-10}$ s at 43°[31]. Once this value is known, it is possible to get correlation times for internal rotation about the C^{α}—C^{β} bond from the NT_1 values of β-carbons. The necessary equation and the resulting correlation times have been reported[31].

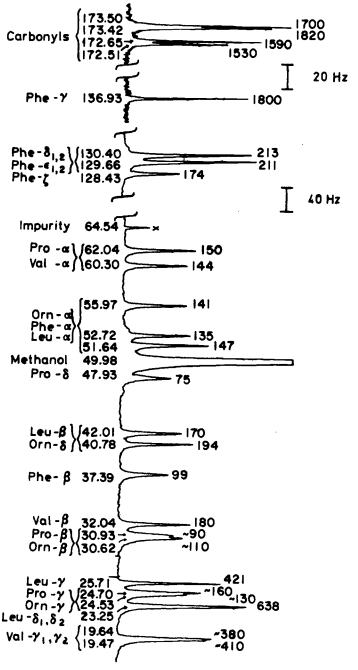

Figure 13. Proton-decoupled natural-abundance ^{13}C NMR spectrum of gramicidin S in methanol (150 mg/ml) at 43°, recorded at 15.18 MHz in a 20 mm tube. Details are given in reference 31. Numbers below each peak are chemical shifts in p.p.m. downfield from Me_4Si. Carbon designations are those of *Figure 14*. Numbers above each peak are T_1 values, in ms.

The NT_1 values of the ^{13}C resonances of neat liquid 1-decanol decrease monotonically as one approaches the hydroxyl end of the molecule[32], because intermolecular hydrogen bonding restricts the mobility at the hydroxyl end of the molecule. Note that equation 5 cannot be used in this case. Each C—H vector changes direction as a result of various internal rotations. The situation is even more complicated in the case of phytol (*Figure 12*). In the first place, T_1 values of non-protonated carbons are much longer than those of protonated ones which have comparable values of τ_{eff}[27]. For this reason, the T_1 of C-3 is much longer than that of its protonated neighbours on the main chain. Second, branching along a hydrocarbon chain and the presence of an olefinic bond cause relatively localized changes in the barriers to internal rotation about C—C bonds[34]. As a result, even though the general trend is for $1/\tau_{eff}$ (and NT_1) of the phytol carbons to increase when going from C-1 to C-16, there are localized deviations (*Figure 12*). For example, C-1 and C-3a have longer NT_1 values than C-2 and C-7a, respectively, as a result of

the relatively low barrier to internal rotation about a C—C bond next to an olefinic carbon[34]. Also, C-7 and C-11 have shorter NT_1 values than C-6 and C-10, respectively, because of increased restrictions to internal rotation accompanying methyl substitution[34].

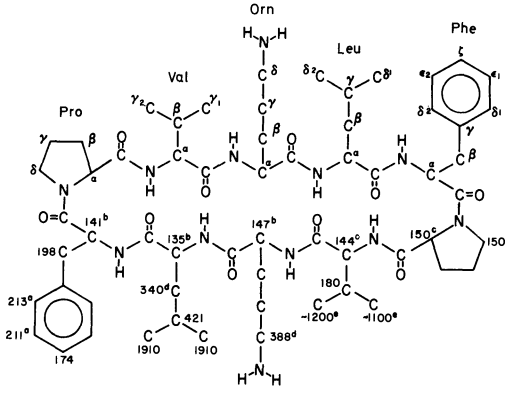

Figure 14. Structure of gramicidin S. Hydrogens bound to carbon have been ommitted. Standard IUPAC–IUB carbon designations are shown in the top portion of the structure. Values of NT_1 (in ms) of protonated carbons are shown in the lower portion. NT_1 values with letter superscripts correspond to carbon resonances that have not been specifically assigned (see *Figure 13*). NT_1 values with the same superscript may have to be interchanged when the corresponding specific assignments become available

PRFT spectra can help the process of specific assignment of ^{13}C resonances, without the need of actually measuring T_1 values. PRFT spectra can be used to distinguish protonated carbons from non-protonated ones[2], or to distinguish protonated carbons that are participating in fast internal rotation from protonated carbons with little internal motion[1,8].

PROTEINS

The ^{13}C—^{1}H dipole–dipole interaction not only contributes to spin–lattice relaxation but also affects the linewidth of each resonance. Even for the smallest proteins in their native conformation, a linewidth of more than 20 Hz at 14.2 kG (slightly less at higher magnetic field strengths) is expected for α-carbons and side-chain protonated carbons not undergoing fast internal rotation. Details have been given elsewhere[28,29,35]. If our aim is to observe resolved single-carbon resonances of a protein, we should determine whether there are any resonances in the ^{13}C spectrum of a native protein that are much narrower than α-carbon resonances. The considerations presented in the previous section indicate that we should consider all non-protonated carbons, and also those protonated carbons that have several degrees of internal freedom. All carbons in the latter category are saturated side-chain carbons that fall in a region of the ^{13}C spectrum crowded with hundreds of protein resonances. Moreover, chemical shift non-equivalence from protein folding, a desirable condition for resolving single-carbon resonances, is least

likely to occur for carbons with appreciable internal mobility. We do not discount the possibility of studying single-carbon resonances of saturated side-chains, especially methyl groups. However, we have concentrated our present efforts in the region of non-protonated carbons. It seems that *non-protonated aromatic* carbons hold the most promise for observing resolved single-carbon resonances, because they cover a relatively large range of chemical shifts for a small number of carbons. The resonances of protonated aromatic carbons are in close proximity to those of many non-protonated ones. However, side-chains of aromatic residues normally do not have appreciable internal rotation[35]. Therefore, on the basis of arguments presented elsewhere[28, 35, 36], we expect that protonated carbons will yield broad resonances that do not seriously interfere with the detection of the narrow non-protonated carbon resonances.

The poor sensitivity of ^{13}C NMR is enough of a problem in dealing with small molecules. With biopolymers it is even more severe. When the extreme narrowing condition (equation 1) does not apply, the NOE is less than 2.988, even if the relaxation mechanism is purely ^{13}C–^{1}H dipolar[28, 29, 36]. Theory predicts[28], and experimental results confirm[35], that aromatic carbons of native proteins normally have an NOE $\lesssim 1.3$, in contrast to the NOE of about 3 normally observed for protonated carbons of organic molecules. Therefore, the aromatic carbons of a 10 mM protein solution will yield resonances with a signal-to-noise ratio less than half that of the ^{13}C resonances of 10 mM sucrose (*Figure 6*), for the same number of spectral scans.

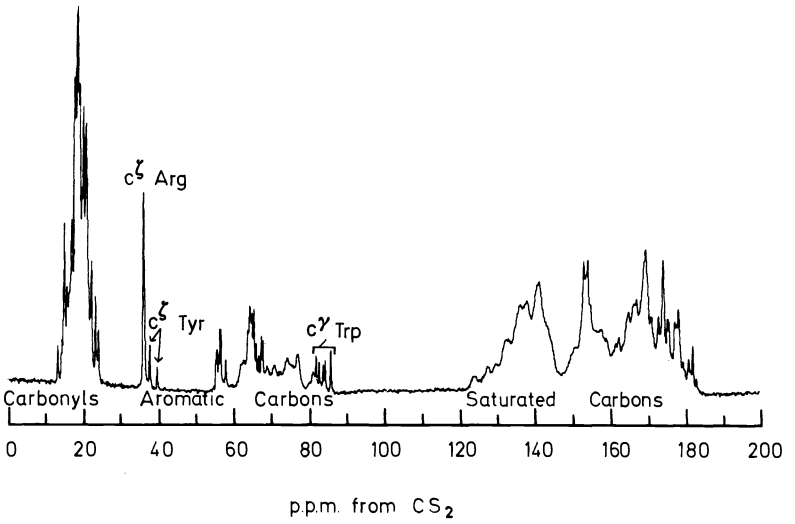

Figure 15. Proton-decoupled natural-abundance ^{13}C NMR spectrum of 13 mM hen egg-white lysozyme (19% w/v in 0.1 M NaCl in H_2O, pH 3.96, 42°C), recorded at 15.18 MHz, with a 20 mm sample tube, 90° rf pulses, 8192 points in the time domain, 1.085 s recycle time, 24 576 accumulations (7.4 h total time), a 250 p.p.m. sweep width and 0.44 Hz broadening from exponential multiplication

Figure 15 shows a proton-decoupled natural-abundance ^{13}C NMR spectrum of 13 mM hen egg-white lysozyme (molecular weight about 14000). This molecule has a total of 613 carbons! Details have been given elsewhere[36, 37]. There are 87 aromatic carbons in a molecule of hen egg-white lysozyme, arising from one histidine, three phenylalanine, three tyrosine and six tryptophan residues. Only 28 of these carbons are non-protonated

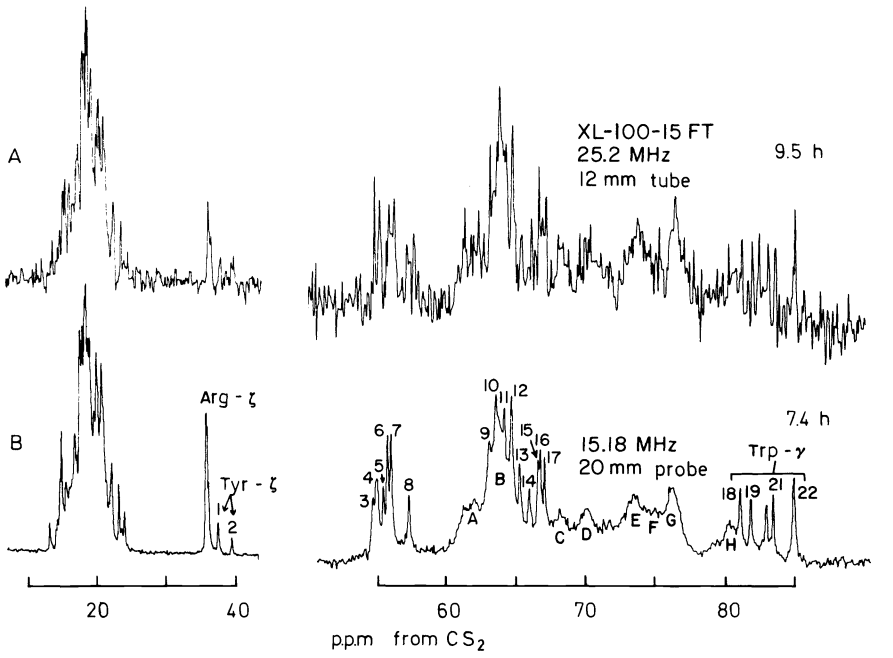

Figure 16. Unsaturated-carbon region of the proton-decoupled natural-abundance ^{13}C Fourier transform NMR spectrum of 13 mM hen egg-white lysozyme (0.1 M NaCl, pH 4, 42°). (A) D_2O solution, recorded at 25.2 MHz on the Varian XL-100-15 Fourier transform NMR spectrometer, with a 12 mm sample tube, 90° rf pulses, 8192 points in the time-domain, 1.035 s recycle time (acquisition time plus delay), 32 768 accumulations (9.5 h total time), a 250 p.p.m. sweep width and 0.6 Hz broadening from exponential multiplication. (B) H_2O solution, recorded at 15.18 MHz on our home-built instrument, with a 20 mm sample tube, 90° rf pulses, 8192 points in the time domain, 1.085 s recycle time, 24 576 accumulations (7.4 h total time), a 250 p.p.m. sweep width and 0.44 Hz broadening from exponential multiplication

ones. *Figure 16B* shows the region of unsaturated carbons of lysozyme, recorded after 7.4 h of signal accumulation. The aromatic region of this spectrum (about 38–85 p.p.m. from CS_2) contains many narrow resonances (peaks 1–22) and a background of broad peaks. On the basis of theoretical considerations[28, 35, 36], we predict that the 28 non-protonated aromatic carbons give rise to peaks 1–22 and that the 59 protonated aromatic carbons produce the broad background. We have verified this expectation experimentally by means of noise-modulated off-resonance proton decoupling, a procedure that selectively broadens protonated carbon resonances[37].

Partial assignments of peaks 1–22 of *Figure 16B* can be made by comparisons with ^{13}C chemical shifts of amino acids and small peptides. For example, the six tryptophan residues yield five C^{γ} resonances (peaks 18–22 of *Figure 16B*) covering a range of about 5 p.p.m. Clearly, peaks 18–21 are single-carbon resonances! Note that the sensitivity of our 20 mm probe greatly facilitates the detection of single-carbon resonances of a protein (compare *Figure 16B* with *Figure 16A*).

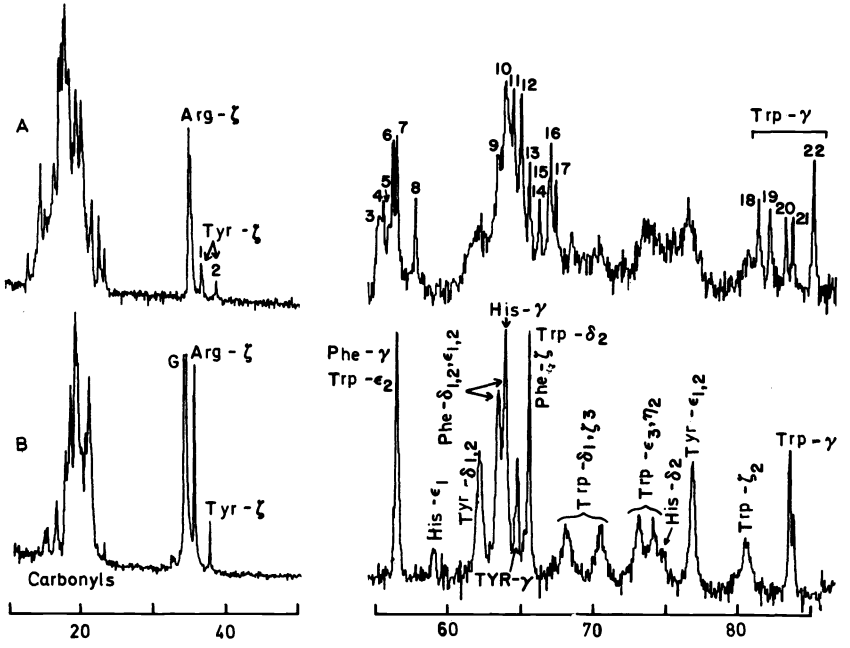

Figure 17. Unsaturated-carbon region in the proton-decoupled natural-abundance ^{13}C Fourier transform NMR spectra of hen egg-white lysozyme (about 15 mM) at 15.18 MHz in a 20 mm sample tube, recorded with 1 Hz digital resolution, after 32 768 accumulations with a recycle time of 1.09 s (9.9 h total time). (A) Native lysozyme, in 0.1 M NaCl, pH 4.0, 42°C. Narrow aromatic carbon resonances, identified by noise-modulated off-resonance proton-decoupling (spectrum not shown), are numbered consecutively from left to right. (B) Guanidine denatured lysozyme, in 0.1 M NaCl and 6.5 M guanidinium chloride, pH 3.9, 54°C. Horizontal scale is in p.p.m. upfield from CS_2. Assignments of non-protonated aromatic carbons are given with horizontal lettering. Assignments of aromatic methine carbons are shown vertically. Standard IUPAC–IUB nomenclature is used for carbon designations

Our results show that folding of a protein into its native conformation can produce large chemical shift non-equivalence of ^{13}C resonances. The six tryptophan residues of denatured lysozyme yield essentially a single C^{γ} resonance (*Figure 17B*). It is only upon folding of the protein into its native conformation that we get five C^{γ} resonances (*Figure 17A*).

Lysozyme is not an isolated example of a protein that yields numerous resolved single-carbon resonances of non-protonated aromatic carbons. We have investigated other proteins[35, 38]. Horse-heart cytochrome *c* has a

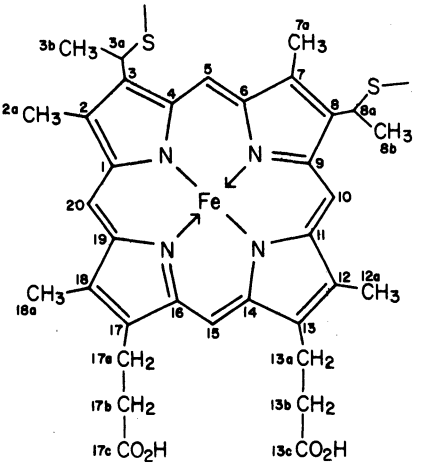

Figure 18. Structure of haem *c*

molecular weight of about 12 000. The structure of its haem is shown in *Figure 18*. Ferrocytochrome *c* is diamagnetic, while ferricytochrome *c* is paramagnetic. Fully proton-decoupled ^{13}C spectra of horse-heart ferricytochrome *c* and ferrocytochrome *c* are shown in *Figures 19A* and *19B*, respectively. The aromatic regions of spectra recorded under conditions of noise-modulated off-resonance proton decoupling are shown in *Figures 20A* and *20B*. In these spectra the broad protonated carbon resonances are further broadened because of inefficient proton decoupling, while the non-protonated

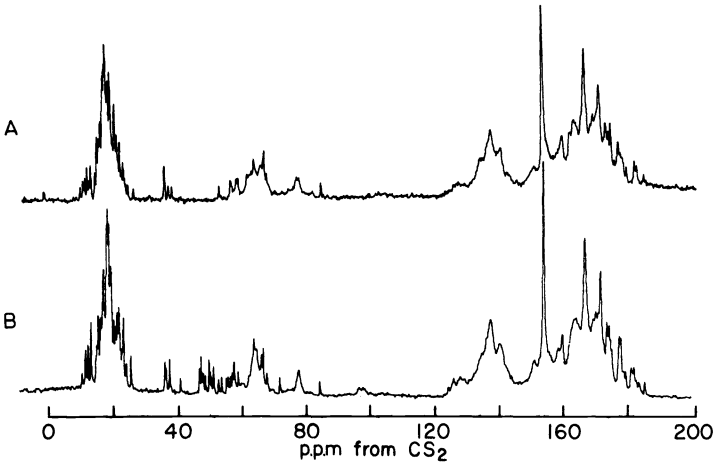

Figure 19. Fully proton-decoupled natural-abundance ^{13}C Fourier transform NMR spectra of horse-heart cytochrome *c* (in 50 mM phosphate buffer (pH 6.7), 41°C), recorded at 15.18 MHz in a 20 mm tube, after 16 384 accumulations (5 h) per spectrum. (A) 8.4 mM ferricytochrome *c*. (B) 11.6 mM ferrocytochrome *c*

carbon resonances are just as narrow as in spectra recorded under conditions of full proton decoupling. In the case of the diamagnetic ferrocytochrome *c* (*Figure 19B*), all 34 non-protonated aromatic carbons, including the 16 non-protonated aromatic carbons of the haem (*Figure 18*), give rise to observable narrow resonances[38]. When going to the paramagnetic ferricytochrome *c* (*Figure 19A*), His-18 (which is coordinated to the iron) and the haem do not yield narrow aromatic carbon resonances[38].

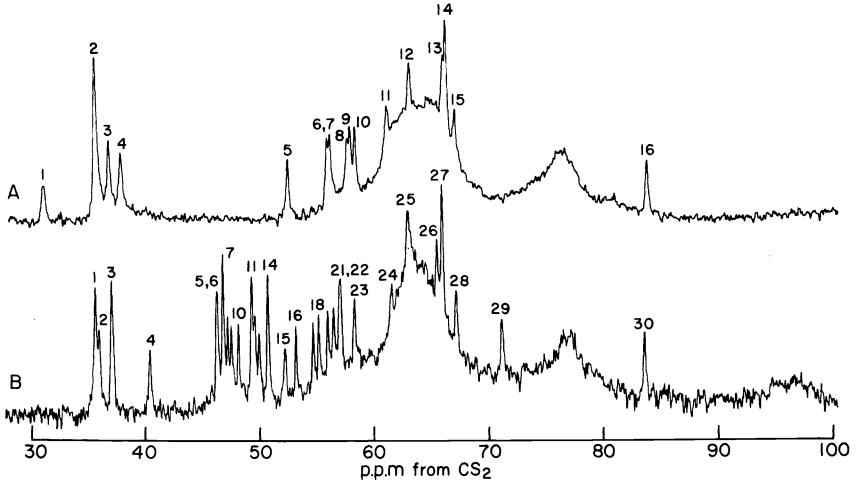

Figure 20. Region of aromatic carbons (and C^{ζ} of the arginine residues) in the noise-modulated, off-resonance, proton-decoupled, natural-abundance ^{13}C Fourier transform NMR spectra of horse-heart cytochrome *c* (in 50 mM phosphate buffer (pH 6.7), 41°C), recorded at 15.18 MHz in a 20 mm tube. (A) 14.4 mM ferricytochrome *c*, after 46 000 accumulations (14 h). (B) 11.5 mM ferrocytochrome *c*, after 16 384 accumulations (5 h)

The observed single-carbon resonances of aromatic amino acid residues can be used, in principle, to monitor the conformational and chemical properties of specific atomic sites of proteins in solution. Such applications will first require the assignment of the resonances to specific points in the amino acid sequence. We are making some progress in this direction[35, 39].

LIPOPROTEINS

Proton-decoupled natural-abundance ^{13}C NMR spectra of aqueous human plasma VLDL, LDL and HDL are shown in *Figure 21*[40, 41]. Most of the prominent features of the lipoprotein spectra arise from the lipid moiety. Resonances are observed for fatty acyl side-chain carbons, for glycerol backbone carbons, for choline carbons, and for ring and side-chain carbons of cholesterol and cholesteryl esters[40, 41]. HDL also yields several narrow peaks that arise from the protein moiety[41]. T_1 values of lipid carbon resonances yield semi-quantitative information about rotational and segmental mobilities of the lipid components[41]. The T_1 values of C-6 of the cholesteryl moiety of HDL and LDL reveal that the fused ring systems occupy regions of much higher microviscosity than that of the aqueous environment[41].

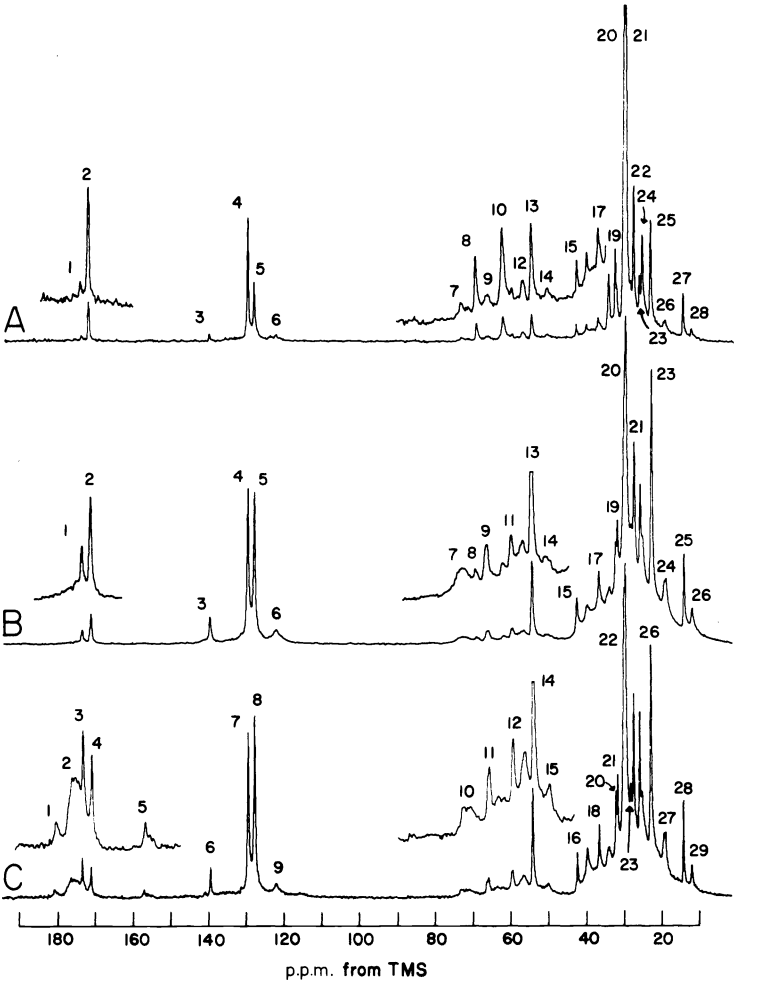

Figure 21. Proton-decoupled natural-abundance ^{13}C Fourier transform NMR spectra of human serum lipoproteins at 36°, recorded at 15.18 MHz in 20 mm sample tubes, with the use of 250 p.p.m. spectral widths, 4096 time-domain addresses and a recycle time of 0.555 s. The inserts were printed with a fourfold vertical expansion. Digital broadening of 0.3 Hz (main spectra) and 2.4 Hz (inserts) was introduced in order to improve the signal-to-noise ratios. Peak numbers are those of reference 41. (A) VLDL, 37 mg/ml, pH 7.5, after 165254 accumulations (25 h). (B) LDL, 110 mg/ml, pH 7.5, after 65536 accumulations (10 h). (C) HDL, 70 mg/ml, pH 8.6, after 65536 accumulations (10 h)

NUCLEIC ACIDS

Because of their low molecular weights (about 25000–30000), tRNAs (*Figure 22*) are attractive choices for initial ^{13}C NMR studies of nucleic acids. We have reported some results on unfractionated tRNA from baker's yeast[42, 43]. With the use of a 13 mm probe[42], the only clearly observed signals

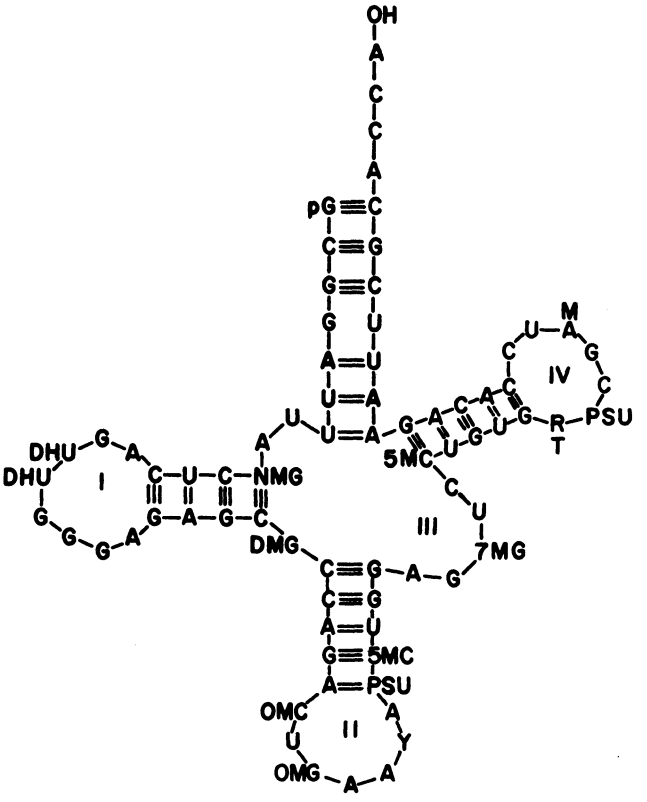

Figure 22. Structure of phenylalanyl tRNA from yeast

were those resulting from the ribose and the four major bases (*Figure 23*). *Figure 24* is a ^{13}C NMR spectrum of unfractionated baker's yeast tRNA recorded with the use of our 20 mm probe[43]. Peaks 2–14 are the resonances of the major base carbons[43]. Peaks 15–19 are the signals of the ribose carbons[43]. Clearly, the ^{13}C NMR spectrum of tRNA is relatively unresolved when compared with the spectrum of a small protein. Nevertheless, there are some weak signals in *Figure 24* that suggest the possibility of observing some single-carbon resonances in ^{13}C NMR spectra of pure strains of tRNA. On the basis of ^{13}C chemical shifts of mononucleosides and mononucleotides[43, 44], some carbons of minor bases (*Figures 25* and *26*) should

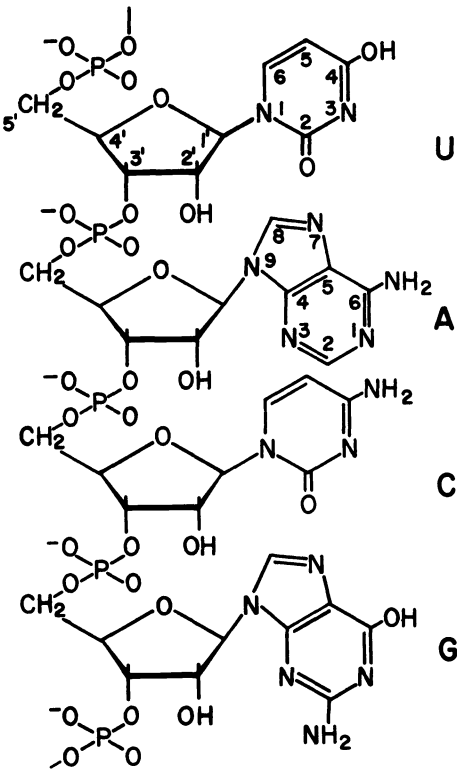

Figure 23. Random segment of a polyribonucleotide chain, showing the four major bases

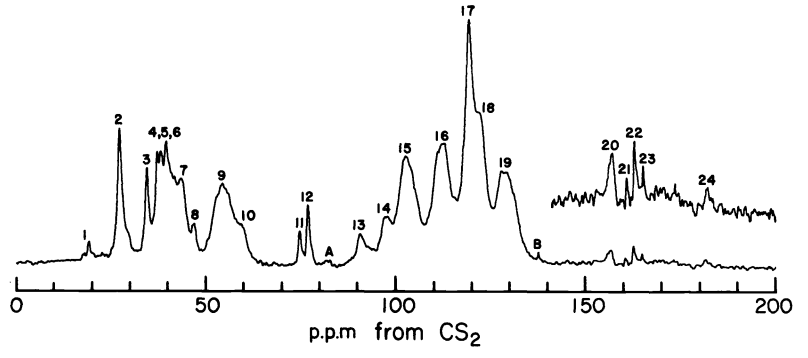

Figure 24. Proton-decoupled natural-abundance ^{13}C Fourier transform NMR spectrum of unfractionated baker's yeast tRNA in water (150 mg/ml), with about 8 Mg^{2+} ions per tRNA molecule, at pH 7.1 and 41°. The spectrum was recorded at 15.18 MHz in a 20 mm tube, after 49 152 accumulations and a recycle time of 1.035 s (14.1 h total time). A digital broadening of 3.1 Hz was used to improve the signal-to-noise ratio. Other details are given in reference 43

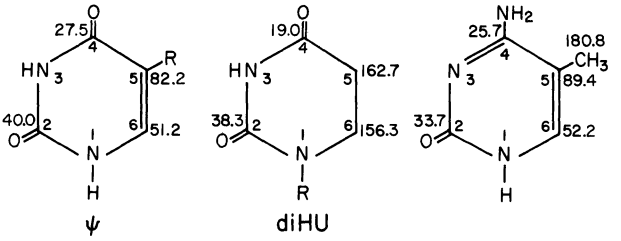

Figure 25. ^{13}C chemical shifts, in p.p.m. upfield from CS_2, of aqueous pseudouridine (ψ), dihydrouridine (diHU) and 5-methylcytosine; R = ribosyl group. Molarities, pH and temperatures were: 0.02, 7.1, 52° (ψ); 0.035, 7.0, 50° (dihydrouridine); 0.20, 6.9, 52° (5-methylcytosine). Other details are given in reference 43

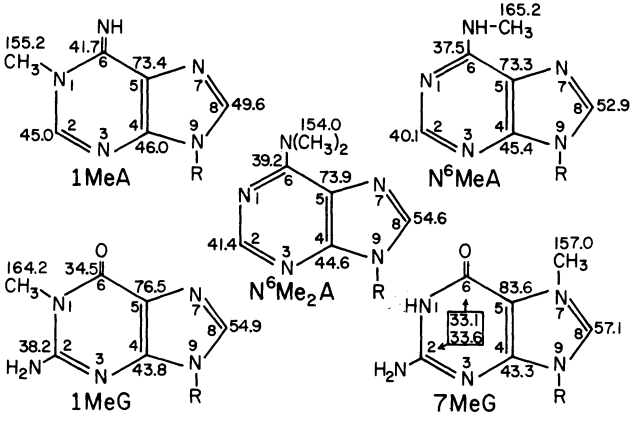

Figure 26. ^{13}C chemical shifts, in p.p.m. upfield from CS_2, of aqueous 1-methyladenosine (1MeA), N^6-methyladenosine (N^6MeA), N^6,N^6-dimethyladenosine (N^6Me_2A), 1-methylguanosine (1MeG) and 7-methylguanosine (7MeG); R = ribosyl group. Molarities, pH and temperatures were: 0.077, 7.1, 42° (1MeA); 0.048, 6.9, 52° (N^6MeA); 0.15, 6.8, 39° (N^6Me_2A); 0.073, 7.0, 51° (1 MeG); 0.073, 7.0, 53° (7 MeG). Other details are given in reference 43

resonate in regions of the spectrum free of interference from ribose and major base resonances[44]. Indeed, peaks 1, A, B, and 20–24 in the spectrum of tRNA (*Figure 24*) have been assigned to minor bases[43].

ACKNOWLEDGEMENTS

This work was supported by the National Science Foundation (Grant GP-40688x), the United States Public Health Service (Grant NS-10977-02) and Eli Lilly and Company.

REFERENCES

[1] R. A. Goodman, E. Oldfield and A. Allerhand, *J. Amer. Chem. Soc.* **95**, 7553 (1973).
[2] D. Doddrell and A. Allerhand, *Proc. Nat. Acad. Sci. US* **68**, 1083 (1971).

[3] J. J. Katz and T. R. Hanson, *Ann. NY Acad. Sci.* **206**, 579 (1973).
[4] S. G. Boxer, G. L. Closs and J. J. Katz, *J. Amer. Chem. Soc.*, **96**, 7058 (1974).
[5] H. J. Reich, M. Jautelat, M. T. Messe, F. J. Weigert and J. D. Roberts, *J. Amer. Chem. Soc.* **91**, 7445 (1969).
[6] D. E. Dorman and J. D. Roberts, *J. Amer. Chem. Soc.* **92**, 1355 (1970); **93**, 4463 (1971).
[7] D. Doddrell and A. Allerhand, *J. Amer. Chem. Soc.* **93**, 2779 (1971).
[8] A. Allerhand and D. Doddrell, *J. Amer. Chem. Soc.* **93**, 2777 (1971).
[9] E. G. Paul and D. M. Grant, *J. Amer. Chem. Soc.* **86**, 2977 (1964).
[10] P. C. Lauterbur, *J. Chem. Phys.* **26**, 217 (1957).
[11] D. M. Grant and E. G. Paul, *J. Amer. Chem. Soc.* **86**, 2984 (1964).
[12] F. J. Weigert, M. Jautelat and J. D. Roberts, *Proc. Nat. Acad. Sci. US* **60**, 1152 (1968).
[13] J. B. Stothers, *Carbon-13 NMR Spectroscopy.* Academic Press; New York (1972).
[14] G. C. Levy and G. L. Nelson, *Carbon-13 Nuclear Magnetic Resonance for Organic Chemists.* Wiley-Interscience; New York (1972).
[15] R. R. Ernst and W. A. Anderson, *Rev. Sci. Instrum.* **37**, 93 (1966).
[16] A. Allerhand, R. F. Childers and E. Oldfield, *J. Magn. Resonance*, **11**, 272 (1973).
[17] M. Rudrum and D. F. Shaw, *J. Chem. Soc.* 52 (1965); R. U. Lemieux and J. D. Stevens, *Can. J. Chem.* **44**, 249 (1966); S. J. Angyal and V. A. Pickles, *Carbohyd. Res.* **4**, 269 (1967).
[18] L. M. J. Verstraeten, *Advan. Carbohyd. Chem.* **22**, 229 (1967).
[19] L. Que and G. R. Gray, *Biochemistry*, **13**, 146 (1974).
[20] T. A. W. Koerner, L. W. Cary, N. S. Bhacca and E. S. Younathan, *Biochem. Biophys. Res. Commun.* **51**, 543 (1973).
[21] A. Jeanes and C. A. Wilham, *J. Amer. Chem. Soc.* **72**, 2655 (1950); A. Jeanes, W. C. Haynes, C. A. Wilham, J. C. Rankin, E. H. Melvin, M. J. Austin, J. E. Cluskey, B. E. Fisher, H. M. Tsuchiya and C. E. Rist, *J. Amer. Chem. Soc.* **76**, 5041 (1954).
[22] A. Allerhand, R. F. Childers, R. A. Goodman, E. Oldfield and X. Ysern, *American Laboratory*, 4 (11), 19 (1972).
[23] A. Allerhand and X. Ysern, unpublished results.
[24] T. C. Farrar and E. D. Becker, *Pulse and Fourier Transform NMR.* Academic Press; New York (1971).
[25] J. R. Lyerla and D. M. Grant, in MTP International Review of Science, Physical Chemistry, Series One, Vol. 4, *Magnetic Resonance*, pp 155–200 (Ed. C. A. McDowell). Butterworths; London: University Park Press; Baltimore (1972).
[26] K. F. Kuhlmann, D. M. Grant and R. K. Harris, *J. Chem. Phys.* **52**, 3439 (1970).
[27] A. Allerhand, D. Doddrell and R. Komoroski, *J. Chem. Phys.* **55**, 189 (1971).
[28] D. Doddrell, V. Glushko and A. Allerhand, *J. Chem. Phys.* **56**, 3683 (1972).
[29] A. Allerhand and E. Oldfield, *Biochemistry*, **12**, 3428 (1973).
[30] S. Berger, F. R. Kreissl and J. D. Roberts, *J. Amer. Chem. Soc.* **96**, 4348 (1974).
[31] A. Allerhand and R. A. Komoroski, *J. Amer. Chem. Soc.* **95**, 8228 (1973).
[32] D. Doddrell and A. Allerhand, *J. Amer. Chem. Soc.* **93**, 1558 (1971).
[33] A. Allerhand, D. Doddrell, V. Glushko, D. W. Cochran, E. Wenkert, P. J. Lawson and F. R. N. Gurd, *J. Amer. Chem. Soc.* **93**, 544 (1971).
[34] J. P. Lowe, in *Progress in Physical Organic Chemistry*, Vol. 6, pp 1–80. Interscience: New York (1968).
[35] E. Oldfield, R. S. Norton and A. Allerhand, in press (1975).
[36] A. Allerhand, R. F. Childers and E. Oldfield, *Ann. N.Y. Acad. Sci.* **222**, 764 (1973).
[37] A. Allerhand, R. F. Childers and E. Oldfield, *Biochemistry*, **12**, 1335 (1973).
[38] E. Oldfield and A. Allerhand, *Proc. Nat. Acad. Sci. US*, **70**, 3531 (1973).
[39] R. S. Norton, R. F. Childers and A. Allerhand, to be published.
[40] J. A. Hamilton, C. Talkowski, E. Williams, E. M. Avila, A. Allerhand, E. H. Cordes and G. Camejo, *Science*, **180**, 193 (1973).
[41] J. A. Hamilton, C. Talkowski, R. F. Childers, E. Williams, A. Allerhand and E. H. Cordes, *J. Biol. Chem.* **249**, 4872 (1974).
[42] R. A. Komoroski and A. Allerhand, *Proc. Nat. Acad. Sci. US*, **69**, 1804 (1972).
[43] R. A. Komoroski and A. Allerhand, *Biochemistry*, **13**, 369 (1974).
[44] D. E. Dorman and J. D. Roberts, *Proc. Nat. Acad. Sci. US*, **65**, 19 (1970).